J Mater Sci (2010) 45:906–910
DOI 10.1007/s10853-009-4019-1

Direct synthesis of mesoporous Fe_3O_4 through citric acid-assisted solid thermal decomposition

Xiaohui Liu · Yong Guo · Yangang Wang · Jiawen Ren · Yanqin Wang · Yanglong Guo · Yun Guo · Guanzhong Lu · Yunsong Wang · Zhigang Zhang

Received: 24 June 2009 / Accepted: 2 November 2009 / Published online: 17 November 2009

Abstract A simple and inexpensive approach to synthesizing mesoporous Fe_3O_4 is developed by using citric acid-assisted solid thermal decomposition of ferric nitrate. The structure and magnetic property of mesoporous Fe_3O_4 were characterized by XRD, FT–IR, N_2 adsorption–desorption isotherms, TEM, and vibrating sample magnetometer. It was shown that the decomposition of citric acid results in the formation of the mesoporous structure and narrow pore-size distribution. The reducing atmosphere which created by the decomposition of the ferric nitrate–citric acid complex caused the partial reduction of Fe(III) to Fe(II) and in turn the formation of Fe_3O_4. Moreover, the strength of the coordination between carboxyl group and Fe^{3+} also affected the phase composition of the iron oxides.

Introduction

Magnetite (Fe_3O_4) is cubic iron oxide with an inverse spinel structure [1]. It has been widely used in a variety of technological applications, such as a catalyst for ammonia, ceramics, energy storage, magnetic data storage, ferrofluids, and bioapplications [2–5]. Various techniques have been developed to synthesize Fe_3O_4, such as the reduction of hematite by H_2 [6], the co-precipitation of ferrous (Fe^{2+}) and ferric (Fe^{3+}) ions [7], microemulsion [8, 9], hydrothermal reaction of $(NH_4)_2SO_4 \cdot FeSO_4 \cdot 6H_2O$ in the presence of hydrazine [10], and the thermal decomposition of organo-metallic compounds [11–14]. Among these methods, the thermal decomposition method has been well accepted as a promising technique to synthesize iron oxides [15, 16]. Typically, this method uses several chemical compounds, including organo-metallic compound, high-boiling temperature solvent, and stabilizing surfactants such as oleic acid and oleylamine. An obvious disadvantage of this method is that most of them involve multiple steps and the synthesized materials often contain expensive surfactants [2]. Here, we report a facile method to synthesis magnetite nanoparticles via solid thermal decomposition reaction of ferric nitrate salt and citric acid, which is a solvent-free, low-temperature, and facile process. Meanwhile, we investigated the role of citric acid in the solid thermal decomposition reaction.

Experimental section

Synthesis

The iron oxides were synthesized using a citric acid-assisted route by the thermal decomposition of ferric nitrate salt in an autoclave at low temperature. All chemicals and reagents used were analytical grade and used without further purification. $Fe(NO_3)_3 \cdot 9H_2O$ and citric acid monohydrate powders were milled separately, and then mixed together. The mixture was transferred into an autoclave and heated at 180 °C for 24 h. The final products were washed with deionized water and dried at 100 °C for 12 h.

Characterization

Powder X-ray diffraction was determined on a Rigaku D-MAX RB X-ray diffractometer at 40 kV and 40 mA,

X. Liu · Y. Guo · Y. Wang · J. Ren · Y. Wang (✉) · Y. Guo · Y. Guo · G. Lu (✉) · Y. Wang · Z. Zhang
Lab for Advanced Materials, Research Institute of Industrial Catalysis, East China University of Science and Technology, Shanghai 200237, People's Republic of China
e-mail: wangyanqin@ecust.edu.cn

G. Lu
e-mail: gzhlu@ecust.edu.cn

and the radiation source was Cu Kα. Infrared spectra of the samples were recorded on a Nicolet Nexus 670 FT-IR spectrophotometer, using the KBr disc-technique. TEM images were obtained with FEI Tecnai 20 S-TWIN. Nitrogen sorption isotherms were measured at 77 K with a NOVA 4200e sorption analyzer. Magnetic properties of the samples are studied by the vibrating sample magnetometer (VSM, Lakeshore, Model 7407) measurement. Thermal gravimetric analysis (TG) and differential thermalgravimetry (DTA) were performed at a heating rate of 10 °C/min from 40 to 500 °C in air flow by PerkinElmer Pyris Diamond using a WCT-2 thermal analyzer.

Results and discussion

Figure 1 is the XRD pattern and FT-IR spectrum of the iron oxide synthesized by the decomposition of the mixture at 180 °C for 24 h, here the molar ratio of ferric nitrate-to-citric acid is 1/1.4. It can be seen from Fig. 1a that the peaks corresponding to magnetite are existed in the sample and no peaks of hematite are detected. The product obtained was further examined by FT-IR spectrometry. The spectrum of the product relating to Fe–O stretch bands is shown in Fig. 1b. In the range of 400–1000 cm^{-1}, the characteristic bands of Fe–O at 580 and 440 cm^{-1} are attributed to the Fe–O stretch bands. The data are consistent with the values reported for Fe_3O_4 in the literature [1]. Therefore, FT-IR result also proved that the composition of the iron oxide is magnetite.

The textural properties of Fe_3O_4 sample were characterized by N_2 adsorption–desorption isotherm (Fig. 2a). It can be seen from Fig. 2a that the isotherm is a type IIb. The broad hysteretic loop from $P/P_0 = 0.45$ to $P/P_0 = 1.0$ is the capillary condensation of flat particles mesopores. The pore-size distribution calculated from BJH model is very narrow as shown in Fig. 2a and the mean mesopore size is about 3.7 nm, the BET surface area and total pore volume are 132 m^{2}g^{-1} and 0.13 cm^{3}g^{-1}, respectively. The mesoporous structure of Fe_3O_4 was further confirmed by transmission electron microscopy (TEM), as shown in Fig. 2b, c. These images show the wormhole-like mesostructure formed with very small Fe_3O_4 particles. In the solid-thermal-decomposition reaction, the introduction of citric acid

Fig. 1 **a** XRD pattern and **b** FT-IR spectrum of Fe_3O_4 synthesized by the decomposition of the mixture (the molar ratio of ferric nitrate/citric acid is 1/1.4) at 180 °C for 24 h

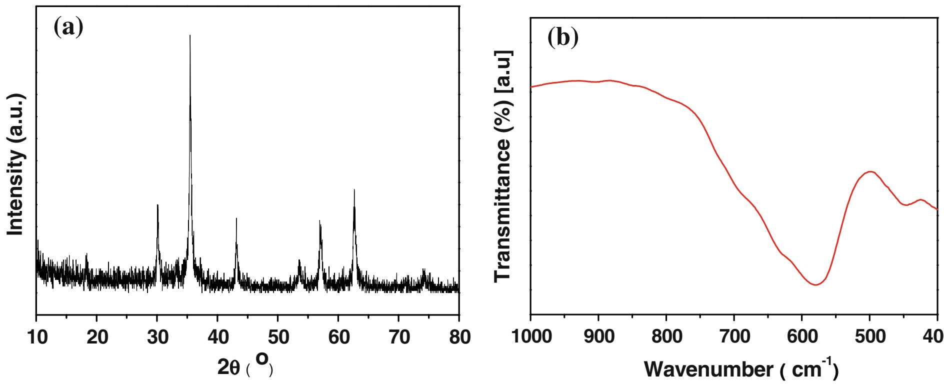

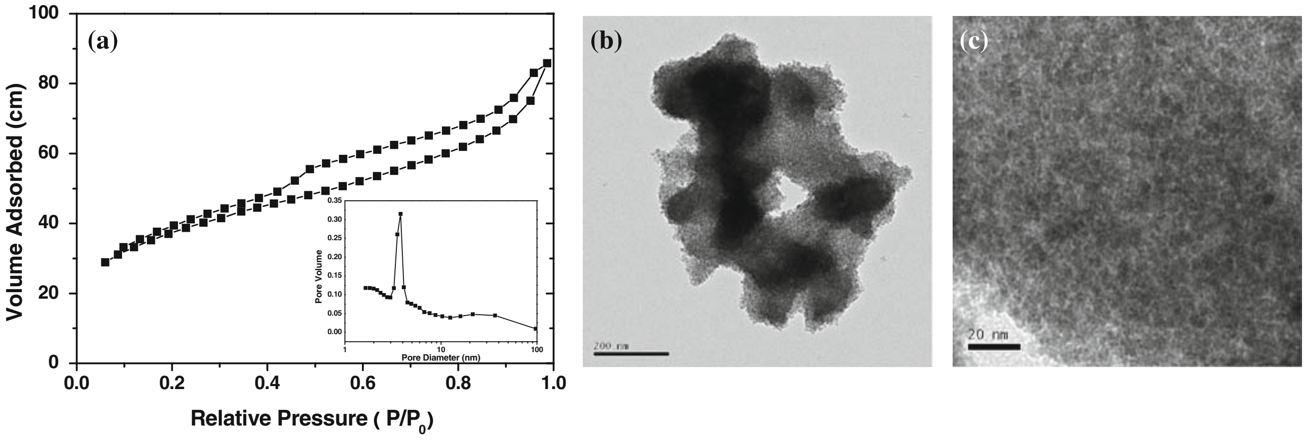

Fig. 2 **a** N_2 adsorption/desorption isotherm and pore-size distribution of Fe_3O_4; **b**, **c** TEM images of Fe_3O_4 synthesized by the decomposition of the mixture (the molar ratio of ferric nitrate -to- citric acid is 1/1.4) at 180 °C for 24 h

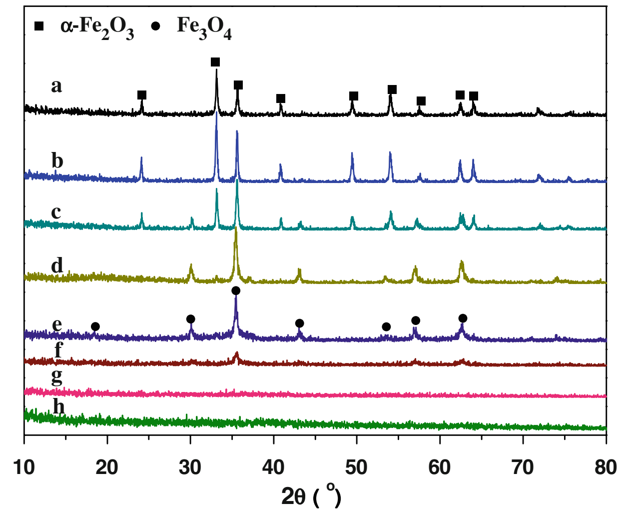

Fig. 3 XRD patterns of the iron oxides in the different ratios of ferric nitrate to citric acid at 180 °C for 24 h: *a* $Fe(NO_3)_3$, *b* 1.0:0.8, *c* 1.0:1.0, *d* 1.0:1.3, *e* 1.0:1.4, *f* 1.0:1.6, *g* 1.0:1.8, *h* ferric citrate

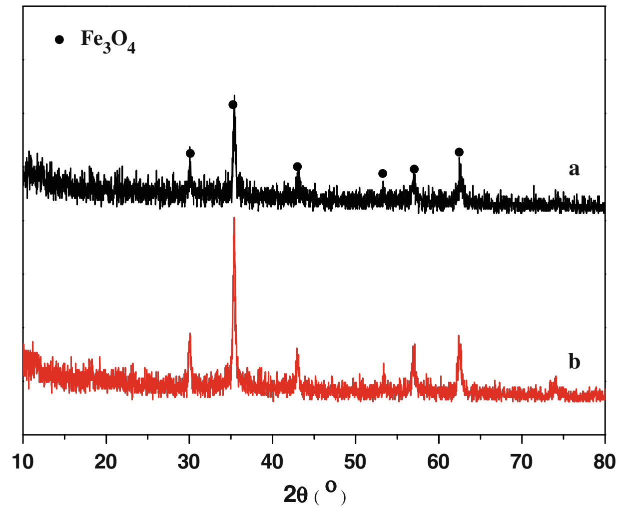

Fig. 4 XRD patterns of iron oxides synthesized at 250 °C for 24 h by decomposition of: *a* ferric citrate, *b* the mixture with the molar ratio of ferric nitrate/citric acid to 1/1.8

effectively disperses ferric nitrate and inhibits the growth of Fe_3O_4 particles. The space occupied with citric acid creates the disordered worm-like pore of iron oxide after the decomposition of citric acid [17].

In order to investigate the influence of citric acid on the composition of iron oxides, the following experiments were carried out and the sample compositions were analyzed by XRD. Figure 3 is the XRD patterns of the samples synthesized by using the solid-thermal decomposition of ferric nitrate, the mixture of ferric nitrate/citric acid and ferric citrate, respectively. It can be seen from Fig. 3 that the peaks corresponding to magnetite exist in the samples synthesized by using citric acid-assisted solid decomposition with different ferric nitrate/citric acid ratio (see Fig. 3c–f). However, using thermal decomposition of ferric nitrate without citric acid, no peaks are corresponding to magnetite and only hematite phase are found (see Fig. 3a.). It should be noted that citric acid is a coordinating agent, which could form a complex by coordinating with Fe^{3+}. This is confirmed by the fact that the mixture color changed from achromatism to brown soon after the addition of citric acid. Considering the coordination action between citric acid and ferric nitrate, the decomposition of ferric citrate at the same condition was carried out, but there was no peak detected, as shown in Fig. 3h. FT-IR analysis also indicated that iron oxide did not form by the decomposition of ferric citrate. This is because the carboxylate-type complexes decompose in the range of 250–350 °C to form simple or mixed oxides [18]. When the decomposition temperature of ferric citrate is raised to 250 °C, the magnetite is formed (see Fig. 4a). So 180 °C is not high enough to form crystallized iron oxides during the thermal decomposition of ferric citrate. This is also proved by the TG/DTA data of ferric citrate in air (see Fig. 5). There are three different weight-loss peaks at the temperature ranges 25–160, 160–200, and 250–350 °C. The first weight loss peak corresponds to the removal of adsorbed water. The second is mainly attributed to the desorption of crystal water in the salt. The third one is ascribed to the decomposition of ferric citrate to form iron oxides due to heating at high temperature.

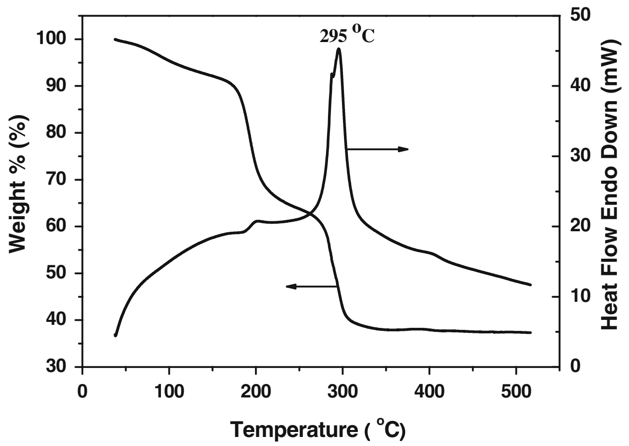

Fig. 5 TG and DTA thermal curves of ferric citrate

Figure 3 also shows the XRD patterns of the iron oxides with different molar ratios of ferric nitrate to citric acid at 180 °C for 24 h. With the increase of citric acid amount, the intensity of hematite diffraction peaks decreases and the intensity of magnetite diffraction peaks increases. When the molar ratio of ferric nitrate-to-citric acid reached 1/1.4, the hematite phase disappeared completely. This indicates that the addition of citric acid affected the phase composition of the iron oxides. While increasing the citric acid amount, an amorphous phase appears. This may be due to the coordination between citric acid and Fe^{3+} becomes stronger with increasing the amount of citric acid. So it is hard to form crystallized iron oxides at 180 °C. When the decomposition temperature is raised to 250 °C, the magnetite is formed (see Fig. 4b). This behavior is in accordance with the decomposition of ferric citrate to iron oxide above 250 °C.

From what is discussed above, the addition of citric acid is the key factor to the formation of Fe_3O_4 in this citric acid-assisted route. Without the addition of citric acid, the final product is hematite, even when other experimental conditions are kept the same. The formation of Fe_3O_4 particles is induced by the partial reduction of Fe(III) to Fe(II) and the reducing atmosphere comes from the decomposition of the carboxylate-type complexes related to the citric acid and ferric ions. To further understand the effect of the carboxyl groups from citric acid, we substituted citric acid with EDTA which has four carboxyl groups. Similarly, magnetite was also formed in the product. It is indicated that the coordination between carboxyl and ferric ions is an important factor for the formation of magnetite in the solid-thermal-decomposition process. However, the formation mechanism of Fe_3O_4 still needs to be investigated further.

The magnetic properties of the obtained magnetite nanoparticles were characterized by using vibrating sample magnetometer and shown in Fig. 6. The hysteresis loop was observed and the saturation magnetization (M_s), remanent magnetization (M_r), and coercivity (H_c) were about 46 emu/g, 9 emu/g, and 136 Oe, respectively. The saturation magnetization is lower than that of bulk Fe_3O_4. The magnetic properties of materials are influenced by many factors, such as the size, structure, surface disordering, morphologies, etc. The lower saturation magnetization in this work may be caused by the existence of non-magnetic carbon decomposed from citric acid and the small particle size [19].

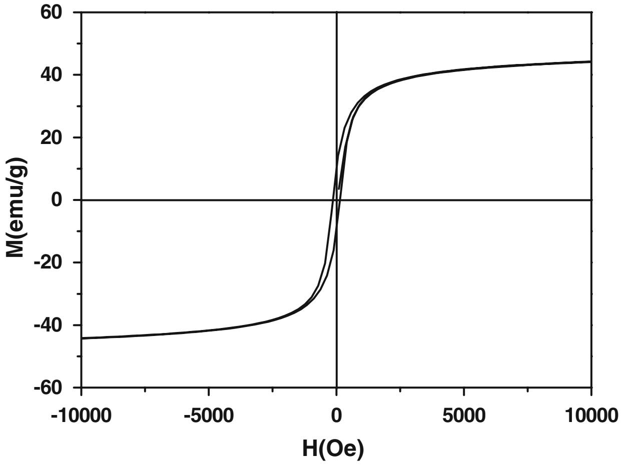

Fig. 6 Magnetization–hysteresis (M–H) loops of the synthesized Fe_3O_4 measured at 300 K

Conclusions

In conclusion, we have succeeded in synthesizing mesoporous Fe_3O_4 by using a citric acid-assisted solid thermal decomposition reaction under mild conditions. The reducing atmosphere, which related to the coordination between citric acid and ferric ions, caused the partial reduction of Fe(III) to Fe(II) and the formation of magnetite. The intensity of the coordination between carboxyl and Fe^{3+} is an important factor for the control of the phase composition. Less citric acid leads to the formation of more hematite phase and more citric acid leads to the formation of amorphous phase. The proper molar ratio of ferric nitrate/citric acid for the formation of pure magnetite (Fe_3O_4) is 1/1.4. At the mean time, the introduction of citric acid effectively dispersed ferric nitrate and inhibited the growth of Fe_3O_4 particles. The space occupied with citric acid created the disordered worm-like pore of iron oxide after the decomposition of citric acid.

Acknowledgements This work was supported financially by the New Century Excellent Talents in University (NCET-05-415), National Natural Science Foundation of China (20673037), the Commission of Science and Technology of Shanghai Municipality (08JC1407900), China.

References

1. Cornell RM, Schwertmann U (1996) The iron oxides: structure, properties, reactions occurrence and uses. VCH, Weinheim
2. Basak S, Rane KS, Biswas P (2008) Chem Mater 20:4906
3. Si SF, Li CH, Wang X, Yu DP, Peng Q, Li YD (2005) Cryst Growth Des 5:391
4. Gaihre B, Khil MS, Ko JA, Kim HY (2008) J Mater Sci 43:6881. doi:10.1007/s10853-008-3003-5
5. Mohapatra S, Pramanik N, Mukherjee S, Ghosh SK, Pramanik P (2007) J Mater Sci 42:7566. doi:10.1007/s10853-007-1597-7
6. Osterhout V (1975) Magnetic oxides. Wiley, New York
7. Caruntu D, Caruntu G, Chen Y, O'Connor CJ, Goloverda G, Kolesnichenko VL (2004) Chem Mater 16:5527
8. Mann S, Sparks HC, Board RG (1990) Adv Microb Physiol 31:125
9. Esquivel J, Facundo IA, Trevino ME, Lopez RG (2007) J Mater Sci 42:9015. doi:10.1007/s10853-007-1834-0
10. Li YD, Liao HW, Qian YT (1998) Mater Res Bull 33:841
11. Matutes-Aquino J, Garcia-Casillasa P, Ayala-Valenzuela O, Garcia-Garcia S (1999) Mater Lett 38:173
12. Sun S, Zeng H (2002) J Am Chem Soc 124:8204
13. Maity D, Choo SG, Yi JB, Ding J, Xue JM (2009) J Magn Magn Mater 321:1256
14. Toniolo J, Takimi AS, Andrade MJ, Bonadiman R, Bergmann CP (2007) J Mater Sci 42:4785. doi:10.1007/s10853-006-0763-7

15. Sun S, Zeng H, Robinson DB, Raoux S, Rice PM, Wang SX, Li G (2004) J Am Chem Soc 126:273
16. Deshpande K, Mukasyan A, Varma A (2004) Chem Mater 16:4896
17. Li L, Yan ZF, Lu GQ, Zhu ZH (2006) J Phys Chem B 110:178
18. Stefanescu M, Stefanescu O, Stoia M, Lazau C (2007) J Therm Anal Calorim 88:27
19. Lu J, Jiao XL, Chen DR, Li W (2009) J Phys Chem C 113:4012